Supporting Information

Enhanced visible-light photocatalytic activity of g-C_3N_4/Zn_2GeO_4 heterojunctions with effective interfaces based on band match

Liming Sun, Yue Qi, Chun-Jiang Jia, Zhao Jin, and Weiliu Fan*

Key Laboratory for Colloid and Interface Chemistry of State Educating Ministry, School of Chemistry and Chemical Engineering, Shandong University, Jinan 250100, China

* To whom all correspondences should be addressed.

Tel: 86-531-88366330, Fax: 86-531-88364864,

E-mail: fwl@sdu.edu.cn

S1. Structures of as-prepared g-C_3N_4 and Zn_2GeO_4

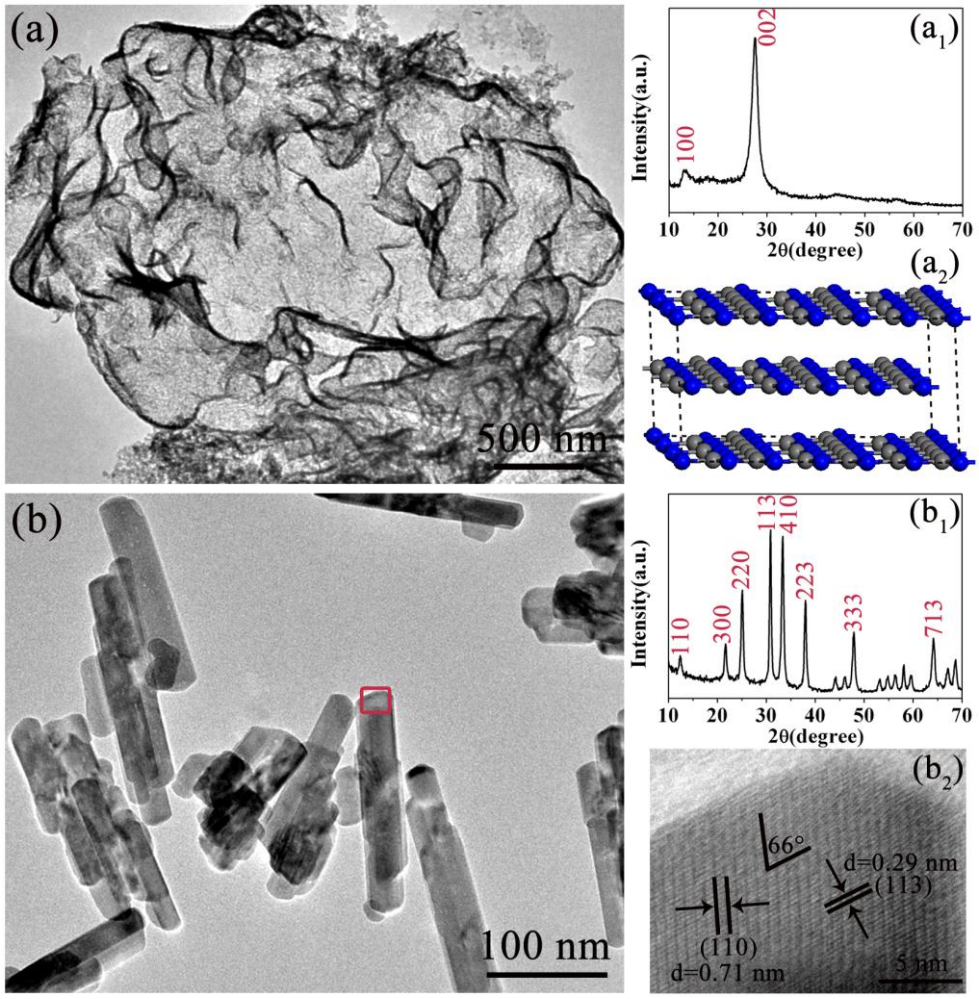

Fig. S1. TEM and XRD of as-prepared g-C_3N_4 (a and a_1) and Zn_2GeO_4 (b and b_1). (a_2) and (b_2) are the schematic of g-C_3N_4 and the HRTEM of Zn_2GeO_4 nanorods, respectively.

From the XRD spectra of g-C_3N_4 (Fig. S1a_1), it can be seen that there are two pronounced diffraction peaks at 13.1° and 27.4°, which can be indexed to the (100) and (002) diffraction planes of the graphite-like carbon nitride, respectively, and correspond to the characteristic inter-layer structural packing and the interplanar stacking peaks of the aromatic systems.[1] As shown in Fig. S1a and a_2, g-C_3N_4 has a crumpled layered structure with several stacking layers along *c*-axis, indicating that the as-prepared g-C_3N_4 plates have exposed (001) surfaces. The XRD patterns of Zn_2GeO_4 (Fig. S1b_1) show that all the diffraction peaks can be assigned exactly to the rhombohedral phase of Zn_2GeO_4 (JCPDS no. 11-0687). The as-prepared Zn_2GeO_4 has

a rod-like shape (Fig. S1b). In the HRTEM of Zn_2GeO_4 nanorods (Fig. S1b$_2$), the lattice fringe of (110) with an interplanar spacing of 0.71 nm is observed parallel to the rod direction, and another lattice fringe of (113) with an interplanar spacing of 0.29 nm is observed at an angle of 66° to the rod direction. This indicates that the Zn_2GeO_4 nanorods grow in the direction of the *c*-axis of the rhombohedral phenacite-type structure[2] and that the exposed side surfaces are (110) surfaces.

S2. Photocatalytic activity of the acetic acid treated and calcined Zn_2GeO_4 and g-C_3N_4:

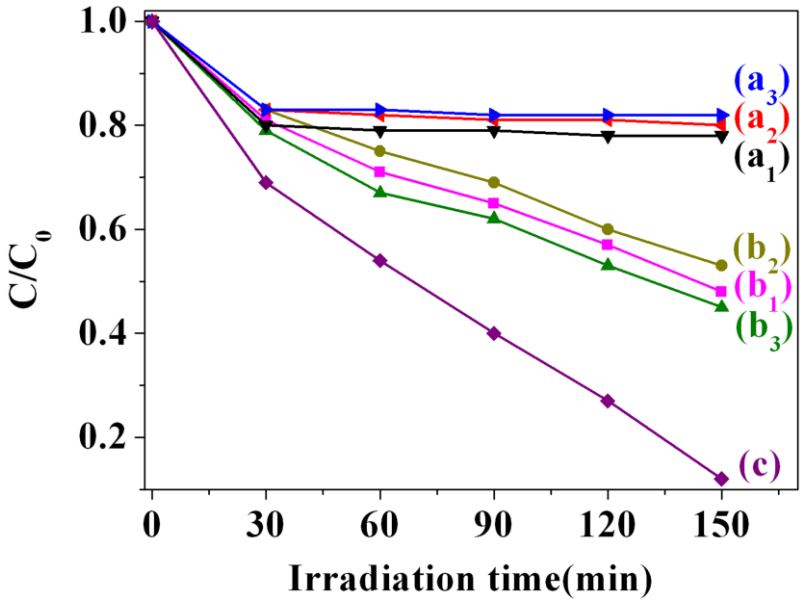

Fig. S2. Photocatalytic degradation of MB over the as-prepared pure Zn_2GeO_4 (a_1), acetic acid treated Zn_2GeO_4 (a_2), 250 °C calcined Zn_2GeO_4 (a_3), pure g-C_3N_4 (b_1), acetic acid treated g-C_3N_4 (b_2), 250 °C calcined g-C_3N_4 (b_3), and OSC 30 wt% g-C_3N_4/Zn_2GeO_4 heterojunctions, respectively.

S3. Stability of the OSC 30 wt% g-C_3N_4/Zn_2GeO_4 heterojunction photocatalysts:

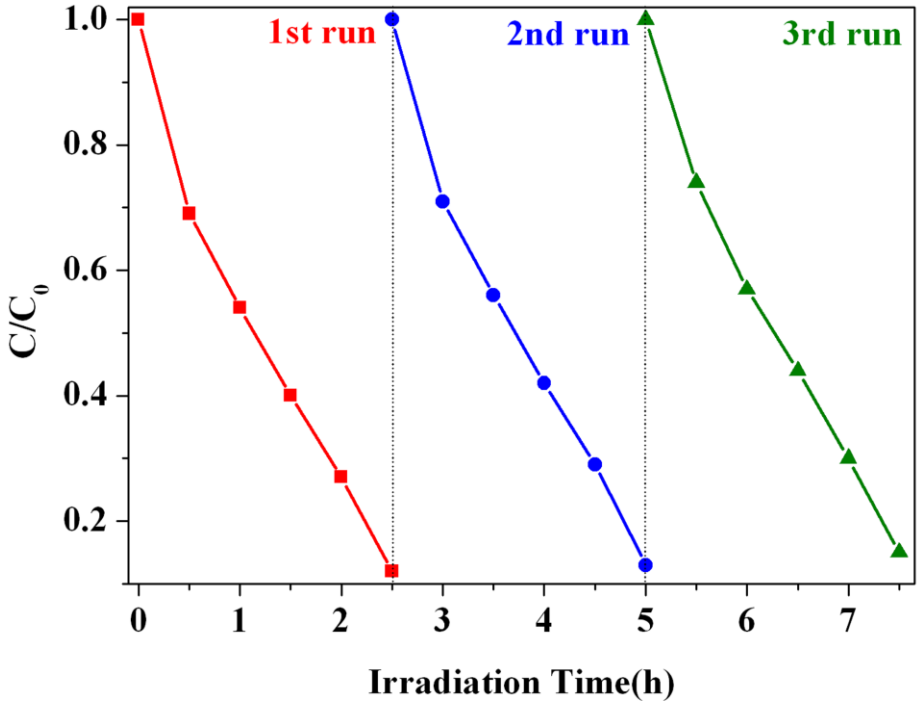

Fig. S3. Recycling test for the photocatalytic degradation of MB on OSC 30 wt% g-C_3N_4/Zn_2GeO_4 heterojunctions under visible light irradiation.

S4. Photocurrents of the acetic acid treated and calcined Zn_2GeO_4 and g-C_3N_4:

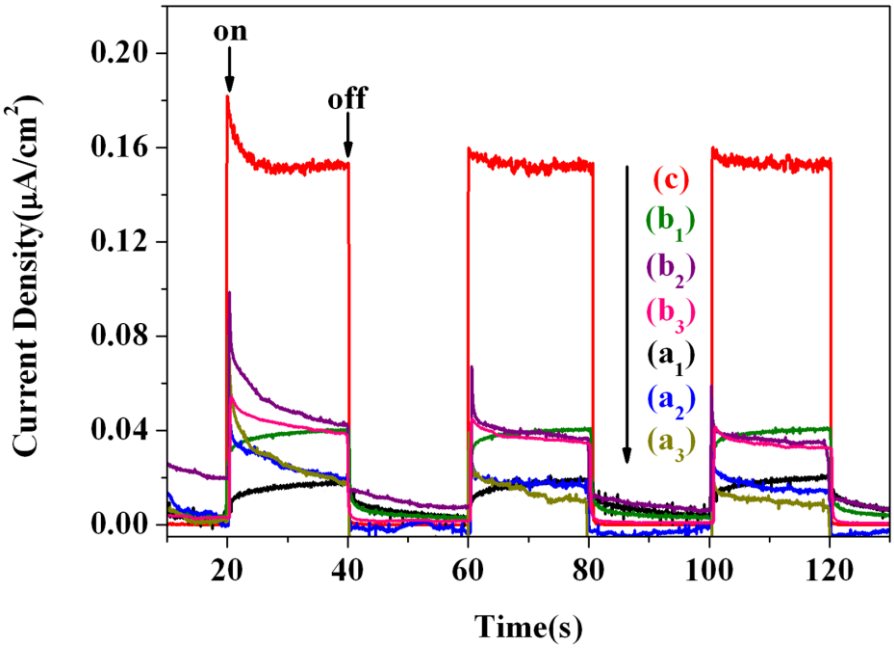

Fig. S4. Photocurrent response of as-prepared pure Zn_2GeO_4 (a_1), 250 °C calcined Zn_2GeO_4 (a_2), acetic acid treated Zn_2GeO_4 (a_3), pure g-C_3N_4 (b_1), 250 °C calcined g-C_3N_4 (b_2), acetic acid treated g-C_3N_4 (b_3), and OSC 30 wt% g-C_3N_4/Zn_2GeO_4 heterojunctions (c) under visible-light irradiation ($\lambda \geq 420$ nm) at 0.5 V *vs* Ag/AgCl.

S5. TEM and HRTEM of g-C_3N_4/Zn_2GeO_4 heterojunctions:

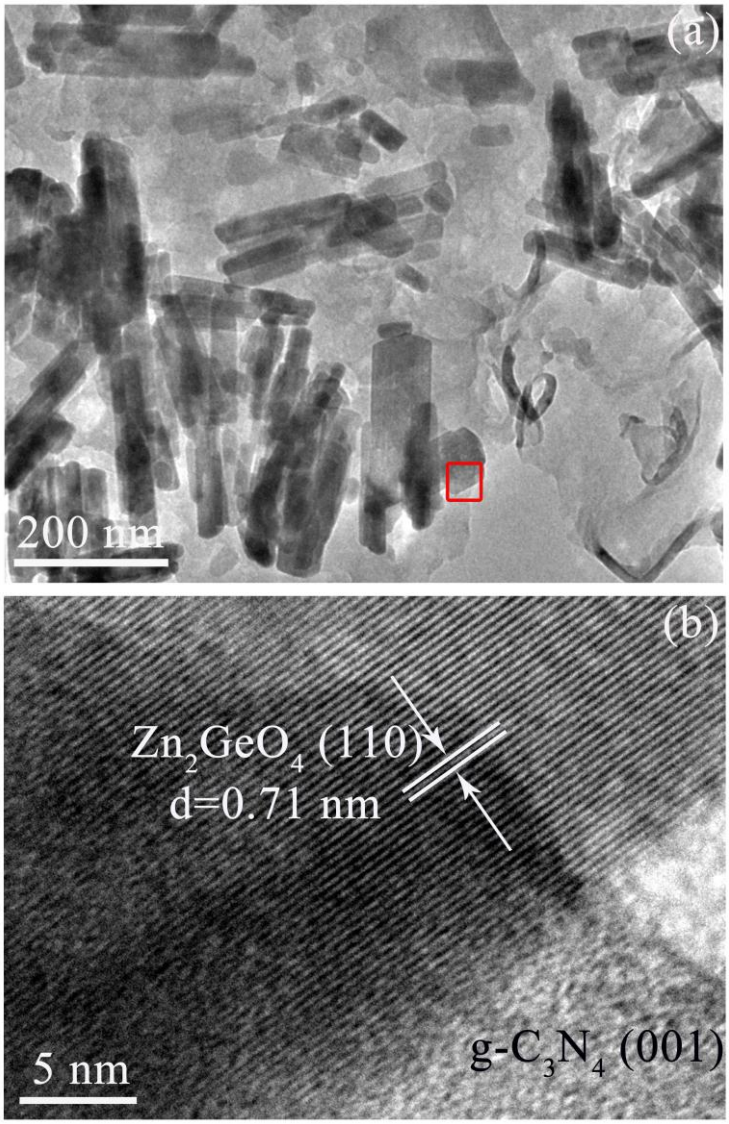

Fig. S5. TEM (a) and HRTEM (b) of the as-prepared g-C_3N_4/Zn_2GeO_4 heterojunctions.

S6. Work functions of g-C_3N_4 (001) surfaces:

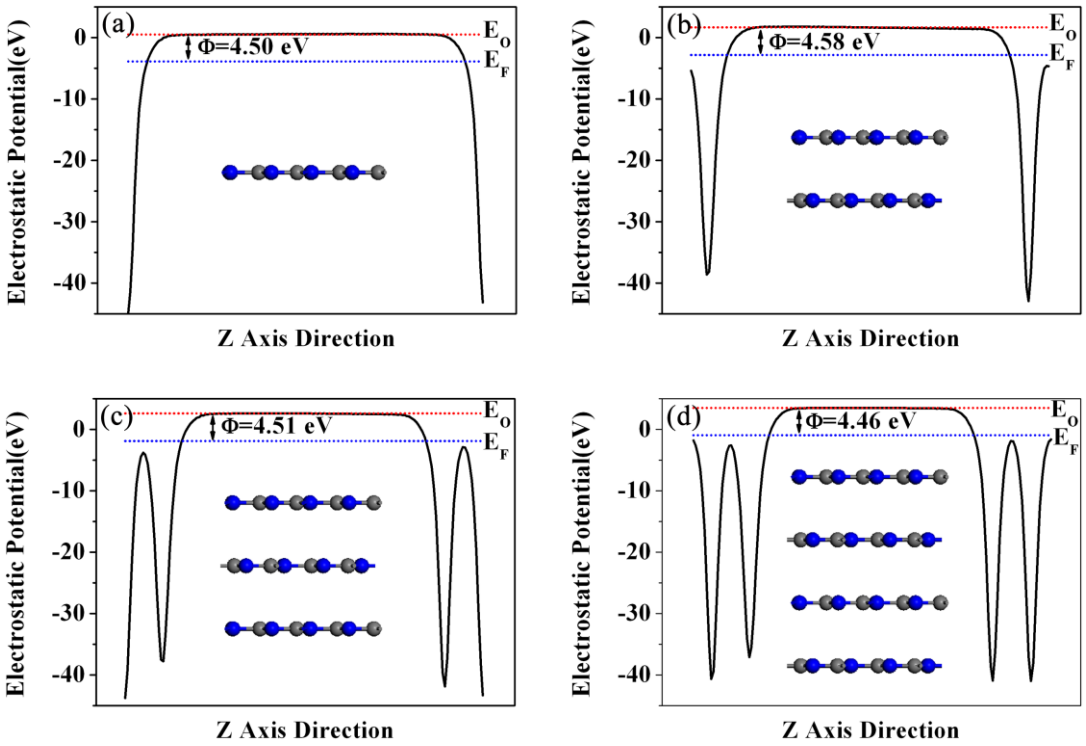

Fig. S6. The electrostatic potentials for g-C_3N_4 (001) surface as a function of the number of C_3N_4 layers: (a) one C_3N_4 layer, (b) two C_3N_4 layers, (c) three C_3N_4 layers, and (d) four C_3N_4 layers. The red and blue dashed lines represent the vacuum level E_O and the Fermi Level E_F, respectively.

S7. UV-vis and VB XPS spectra of g-C_3N_4 and Zn_2GeO_4 individuals:

Fig. S7 shows the UV-vis and valence band X-ray photoelectron spectroscopy (VB XPS) spectra of pure g-C_3N_4 and Zn_2GeO_4. The fundamental absorption edge of g-C_3N_4 is at 474 nm, which can be assigned to a band gap of 2.62 eV (Fig. S7a). Pure Zn_2GeO_4 exhibits an absorption edge of 288 nm corresponding to the band gap of 4.31 eV (Fig. S7c). The positions of the valence band (VB) edge of g-C_3N_4 and Zn_2GeO_4 can be seen at about 1.30 and 3.45 eV_{NHE} (NHE=Normal Hydrogen Electrode) (Fig. S7b and d), respectively, which are consistent with the values reported in literature.[3,4] Because the relationship between E_{NHE} and E_{AVS} (AVS=Absolute Vacuum Scale) is $E_{AVS}=E_{NHE}-E^e$, where E^e is the energy of free electrons in the hydrogen scale (about 4.50 eV), the energies of the VB edge of g-C_3N_4 and Zn_2GeO_4 are estimated to be -5.80 and -7.95 eV_{AVS}, respectively. Based

on the band gap positions, the energies of the CB edge of g-C_3N_4 and Zn_2GeO_4 are determined to be -3.18 and -3.64 eV_{AVS}, respectively.

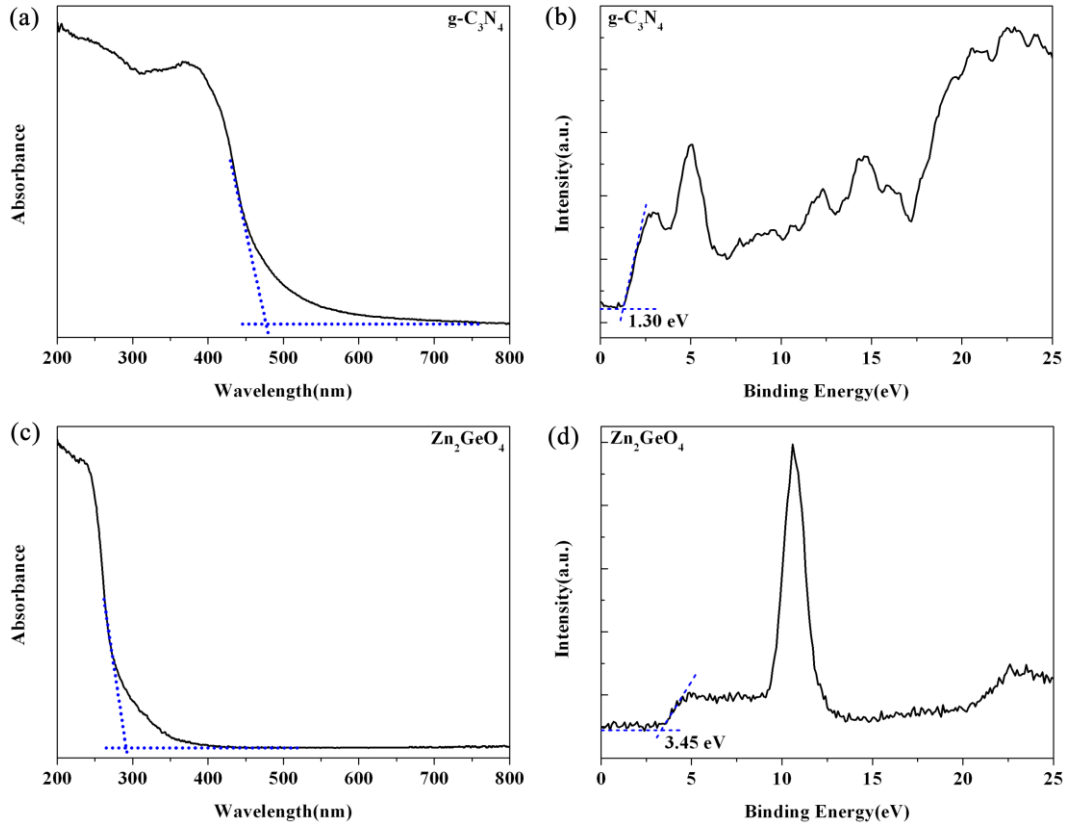

Fig. S7. UV-vis and VB XPS spectra for the pure g-C_3N_4 (a and c) and Zn_2GeO_4 (b and d), respectively.

REFERENCES

1 S. Matsumoto, E. Q. Xie and F. Izumi, *Diamond Relat. Mater.*, 1999, **8**, 1175-1182.

2 S. C. Yan, L. J. Wan, Z. S. Li and Z. G. Zou, *Chem. Commun.*, 2011, **47**, 5632-5634.

3 F. Yang, M. Lublow, S. Orthmann, C. Merschjann, T. Tyborski, M. Rusu, S. Kubala, A. Thomas, R. Arrigo, M. Hävecker and T. Schedel-Niedrig, *ChemSusChem.*, 2012, **5**, 1227-1232.

4 N. Zhang, S. X. Ouyang, P. Li, Y. J. Zhang, G. C. Xi, T. Kako and J. H. Ye, *Chem. Commun.*, 2011, **47**, 2041-2043.